Collection efficiency and charge transfer optimization for a 4-T pixel with multi n-type implants*

Li Weiping(李伟平), Xu Jiangtao(徐江涛)†, Xu Chao(徐超), Li Binqiao(李斌桥), and Yao Suying(姚素英)

School of Electronic and Information Engineering, Tianjin University, Tianjin 300072, China

Abstract: In order to increase collection efficiency and eliminate image lag, multi n-type implants were introduced into the process of a pinned-photodiode. For the purpose of improving the collection efficiency, multi n-type implants with different implant energies were proposed, which expanded the vertical collection region. To reduce the image lag, a horizontal gradient doping concentration eliminating the potential barrier was also formed by multi n-type implants. The simulation result shows that the collection efficiency can be improved by about 10% in the long wavelength range and the density of the residual charge is reduced from 2.59×10^9 to 2.62×10^7 cm^{-3}.

Key words: CMOS image sensor; photodiode; collection efficiency; charge transfer; image lag

DOI: 10.1088/1674-4926/32/12/124008 **EEACC:** 2550X; 7230G

1. Introduction

Pinned photodiodes (PPDs) were first used in CCD image sensors and introduced into the CMOS image sensor (CIS) process by the Eastman Kodak Company in 1995. By separating the charge storage region from the Si/SiO_2 interface, blue light response and the characteristic of dark current are both improved[1, 2]. CIS has many advantages over CCD image sensors such as lower power consumption, lower cost and higher level of integration. In recent years, the market of CIS is already bigger than the market of CCD, especially in high reliability and radiation-resistant applications[3, 4].

A traditional PPD structure is formed by a single implant of n-type impurities. Collection efficiency of red light is low because the depletion depth is limited by the requirement of complete charge transfer. Adjusting the energy and the dose of an n-type ion implant can form a deeper N/P-sub junction, but these adjustments are limited by the requirement of complete charge transfer. Lower concentration of p substrate will also help, but the characteristics of the whole circuit will be affected. Forming stratified doping arrangement by implanting p-type impurities into the n region can improve the collection efficiency. However, this kind of process is complicated and hard to control. Using two or more n-type ion implants with different impurity species, energies and doses is also helpful[5−7].

During charge transfer, some of the electrons are likely to be trapped in the middle of the N region. The condition worsens when the size of the pixel gets bigger. This problem can be solved by changing the shape of the PPD at the cost of introducing fixed-pattern noise (FPN) and lowering the fill factor of the pixel[8, 9].

An optimization method with multi n-type implants is presented in this paper to improve the collection efficiency of the photodiode, especially for long wavelength light. Charge transfer is also improved by forming a gradient doping distribution in the buried n region. All the optimizations are simulated with computer analysis tool Sentaurus-TCAD.

2. Charge collection and transfer

All improvements in this paper are based on CMOS 4 transistor (4T) pixel structure. A schematic view of 4-T CIS pixel cell is shown in Fig. 1. The four transistors are transfer gate (TG), source follower (SF), reset transistor and row select transistor (SEL)[10].

The PPD structure is composed of an n-layer in the p substrate and a p-layer at surface. Signal electrons are generated by light incident on the PPD. At the beginning of the collection, the N-type region is fully depleted. Figure 2 presents the potential profile along line AA' in Fig. 1. The beam-generated electrons are collected in the N region. After the integration time, the signal electrons will be transferred to the FD node

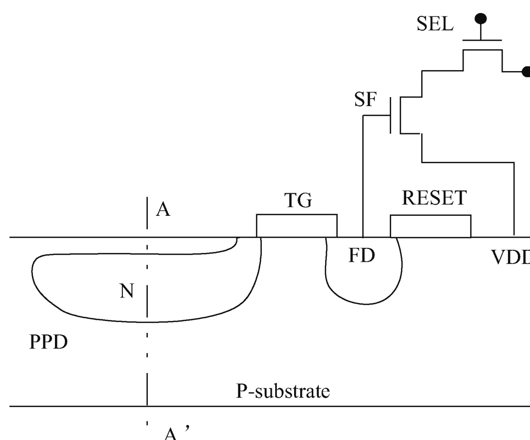

Fig. 1. Schematic view of 4T CIS pixel.

* Project supported by the National Natural Science Foundation of China (Nos. 61036004, 60976030).
† Corresponding author. Email: xujiangtao@tju.edu.cn
Received 13 June 2011, revised manuscript received 20 July 2011
© 2011 Chinese Institute of Electronics

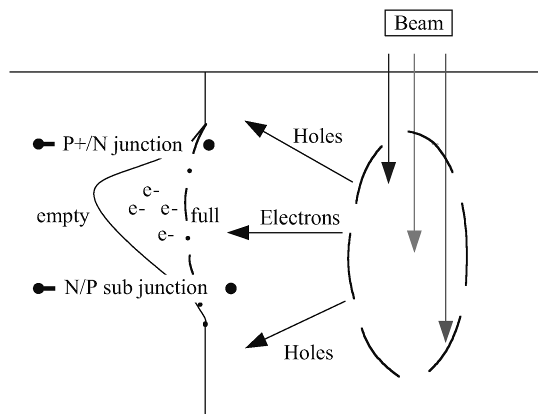

Fig. 2. PPD potential profile.

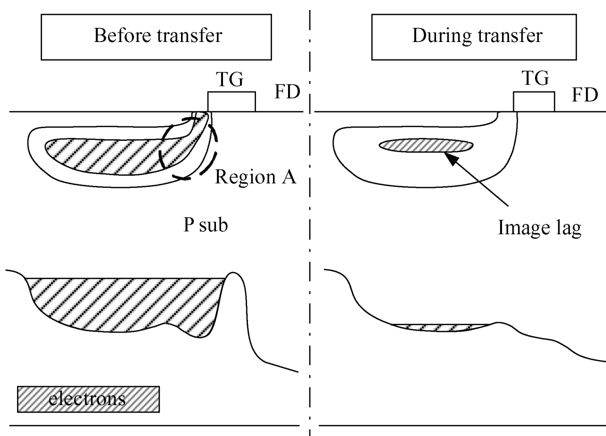

Fig. 3. Potential diagram before and during charge transfer.

and then read out through SF and SEL as voltage signal.

The wavelength of visible region is 0.4–0.8 μm, the absorption length varies from 0.1 to 10 μm[11]. Electrons generated in the depleted region will be easily captured by the n region under the effect of the electric field. However, photons with a long wavelength penetrate deep into the substrate and the electrons generated there will exist as minority carriers. The diffusion behavior of the minority carriers greatly affects the image sensor characteristics. Minority carriers can diffuse to adjacent photodiodes through the substrate and cause image blurring. Since the absorption length of long wavelength light is much longer than short wavelength light, the absorption of long wavelength light is important for reducing image blurring.

Complete transfer of electrons is necessary for the purpose of reducing the random noise. However, sometimes a potential barrier in region A as shown in Fig. 3 will stop the electrons from complete transfer. Region A connects n-layer and TG channel. When the length of the transfer gate is 0.5 μm or even shorter, the depletion of region A is likely to be affected by the p-type anti punch through (APT) implantation between PPD and FD node. If region A depleted faster than the area away from the TG channel, a potential barrier will exist in region A. As a result, some of the signal electrons will remain in the n region as image lag and this does not fit the requirement of complete charge transfer.

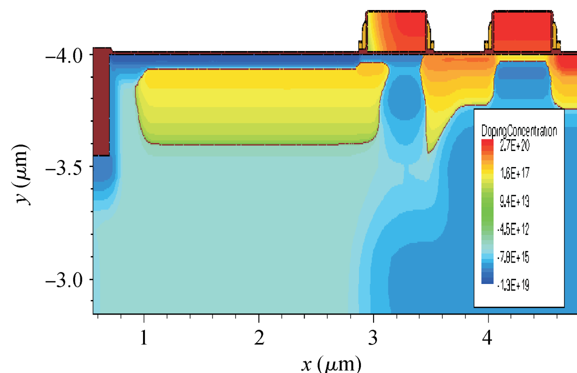

Fig. 4. PPD structure with one n-layer.

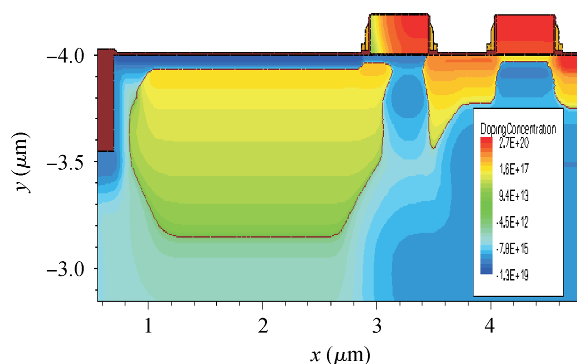

Fig. 5. PPD structure with two n-layers connecting each other.

3. Optimization for the collection efficiency

An additional n-type implant is introduced into the process of 4T pixel to form a second n-type doping region right below the first n-type doping region. These two n-type doping regions connect to each other so the depletion region is expended in vertical direction and the absorption of long wavelength light is improved.

Figures 4 and 5 present the structures that used in the simulation. The length of PPD is 2.0 μm, and the length of the transfer gate is 0.5 μm. Source follower transistor and row select transistor are removed from the pixel structure as they do not affect the light absorption nor the charge transfer. Figure 4 shows the doping profile of the prior art whose n-layer was formed by a single implant of phosphorus. The doping concentration of the substrate is 1×10^{15} cm^{-3}. The n and p-layer of the PPD was formed by implantation with a dose of 4×10^{12} cm^{-2} and 5×10^{13} cm^{-2}, respectively. The implantation energy of n-layer is 50 keV. Figure 5 shows the optimized pixel structure with an additional n-layer formed under the first n-layer. Implantation profile of the first n layer in Fig. 5 is exactly the same as the structure in Fig. 4. The energy of the second implant is 300 keV and the dose is 2×10^{11} cm^{-2}. These two n-layers are formed with the same pattern. Figure 6 shows the doping concentration of these two structures at $x = 2.0$ μm. The width of the n region in vertical direction was expended with the additional n-type implant.

In order to shorten the simulation time strong incident beam intensity and short integration time is specified in the simulation. It has been tested that the same simulation result

Table 1. Signals at different wavelengths.

WL (nm)	1L: V_{rst} (V)	2L: V_{rst} (V)	1L: V_{sig} (V)	2L: V_{sig} (V)	1L: $V_{rst} - V_{sig}$ (V)	2L: $V_{rst} - V_{sig}$ (V)	Improved (%)
500	2.28981	2.28675	2.08254	2.07506	0.20727	0.21475	3.61
600	2.28981	2.28675	2.08094	2.06431	0.20887	0.22244	6.50
700	2.28981	2.28675	2.14587	2.13048	0.14394	0.15627	8.57
800	2.28981	2.28675	2.20774	2.19684	0.08207	0.08991	9.55
900	2.28981	2.28675	2.27916	2.27511	0.01065	0.01164	9.30

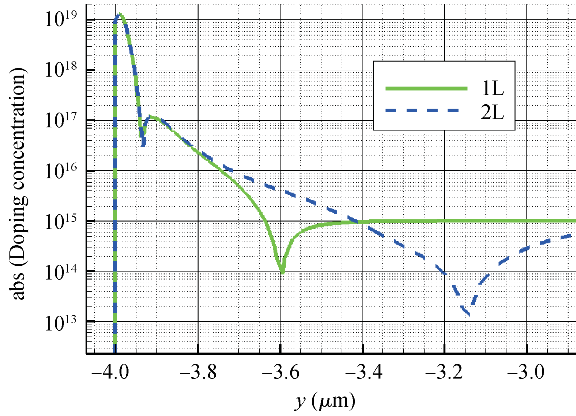

Fig. 6. Comparison of doping profile at $x = 2.0$ μm.

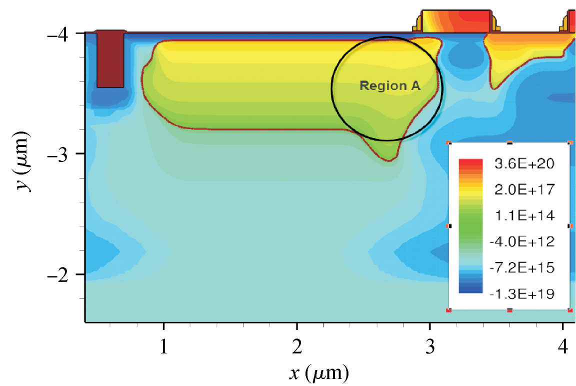

Fig. 7. Doping concentration diagram with the implantation in region A.

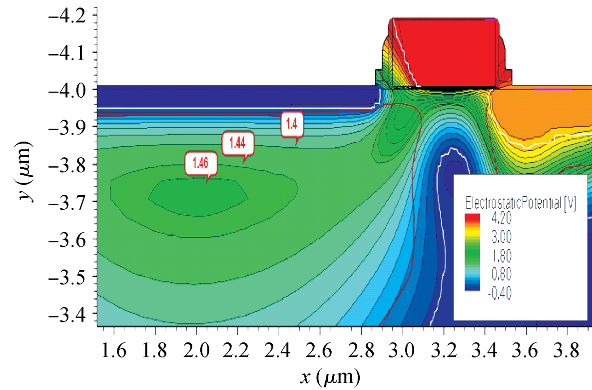

Fig. 8. Electrostatic potential diagram of the double n-layer pixel during charge transfer.

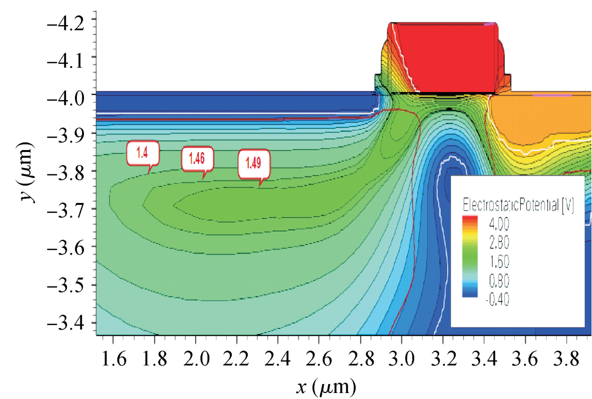

Fig. 9. Electrostatic potential diagram of the optimized one during charge transfer.

will be obtained with different beam intensity and integration time as long as the total amount of incident photons of different simulations are exactly the same. Integration time in the simulation is set to 5 μs. Incident beam intensity is set to 1×10^{16} cm^{-2}·s, and the wavelength range is varied from 500 to 900 nm. After the integration time, TG voltage is set to 3.3 V and signal electrons will be transferred from PPD to FD which was reset to a high voltage earlier. The voltage of FD was recorded in Table 1.

The simulation result shows that the collection efficiency of the pixel is improved especially in long wavelength range.

4. Optimization for charge transfer

Potential pocket and potential barrier existing around the channel of TG have been studied a lot. In this section of the paper, the barrier previously shown in Fig. 3 was optimized by another implant of phosphorus at region A. The energy of the implant is 250 keV and the dose is 3.5×10^{11} cm^{-2}. Doping concentration in region A is higher than the other part of the n region as shown in Fig. 7 and this makes sure that region A will not be depleted until the depletion of the whole n region. The optimization is based on double n-layer PPD structure previously shown in Fig. 5. Figure 8 shows the potential diagram of double n-layer PPD structure during charge transfer and Figure 9 is for the pixel that have been optimized. According to the simulation result shown in these two figures, the barrier in region A was reduced.

As the barrier in region A is removed, the electrons collected in n region can be pulled out more easily than the one without optimization. Electron density of the transferring state at coordinate $y = -3.7$ is shown in Fig. 10. Max electron density in n-layer drops from 2.59×10^9 to 2.62×10^7 cm^{-2}. With the optimization in region A the depletion of n region is greatly improved.

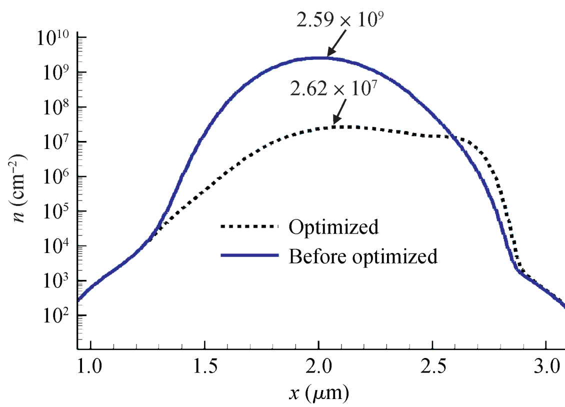

Fig. 10. Electron density at $y = -3.7$.

5. Conclusion

Multi n-type implants are introduced into the pixel process. The PPD structure formed by this process has a wide n region deep in the p substrate and a horizontal gradient doping concentration in the n-layer. Compared with the traditional PPD structure formed by an implant of n-type impurities, electrons generated by red light are more likely to be captured by the double n-layer PPD and the electrons can be pulled out more easily with the gradient doping concentration in n-layer. The simulation result shows that the absorption of long wavelength light can be improved by 9.55%. Compared with the double n-layer PPD, the residual electron density of the PPD with gradient doping concentration in the n-layer can be reduced to about 1% of the previous level. The additional implants can be added into any pixel process at the expense of one more mask. The simulation results provide an easy method for the pixel designer to improve the performance of the pixel.

References

[1] McColgin W C, Lavine J P, Kyan J, et al. Dark current quantization in CCD image sensors. IEDM Tech Dig, 1992: 113

[2] Lee P P, Guidash R M, Stevens E G, et al. Active pixel sensor integrated with a pinned photodiode. USA Patent, No. 5625210, 1997

[3] Nakamura J. Image sensors and signal processing for digital still cameras. Boca Raton, FL: CRC Press, 2006: 90

[4] Yu Junting, Li Binqiao, Yu Pingping, et al. Two-dimensional pixel image lag simulation and optimization in a 4-T CMOS image sensor. Journal of Semiconductors, 2010, 31(9): 094011

[5] Stevens E G. Photodetector structure for improved collection efficiency. USA Patent, No. 20070069260A1, 2007

[6] Rhodes H E. Image sensor pixel having photodiode with multi-dopant implantation. USA Patent, No. 007670865B2, 2010

[7] Hynecek J. Stratified photodiode for high resolution CMOS image senor implemented with STI technology. USA Patent, No. 20100044824A1, 2010

[8] Patterson J J, Swenson M S, Dowley C I. Electronic components and methods for improving pixel charge transfer in the electronic component. USA Patent, No. 006476426B1, 2002

[9] Shin B, Park S, Shin H. The effect of photodiode shape on charge transfer in CMOS image sensors. Solid-State Electron, 2010, 54: 1416

[10] Xu Jiangtao, Yao Suying, Li Binqiao, et al. Design, analysis, and optimization of a CMOS active pixel sensor. Chinese Journal of Semiconductors, 2006, 27(9): 1548

[11] Ohta J. Smart CMOS Image sensors and applications. Boca Raton, FL: CRC Press, 2008: 12